Yu Xuan (Orcid ID: 0000-0002-9055-7923)
Seyfferth Angelia Lyn (Orcid ID: 0000-0003-3589-6815)
Michael Holly A (Orcid ID: 0000-0003-1107-7698)

# Using hydrological-biogeochemical linkages to elucidate carbon dynamics in coastal marshes subject to relative sea-level rise

**Julia A. Guimond[1], Xuan Yu[1,2], Angelia L. Seyfferth[1,3], and Holly A. Michael[1,4*]**

1. Department of Geological Sciences, University of Delaware, Newark DE 19716, USA.
2. School of Civil Engineering, Sun Yat-sen University, Guangzhou 510275, China.
3. Department of Plant and Soil Sciences, University of Delaware, Newark, DE 19716, USA.
4. Department of Civil & Environmental Engineering, University of Delaware, Newark DE 19716, USA.

*Corresponding author: Holly A. Michael (hmichael@udel.edu)

**Key Points:**

- Hydrological-biogeochemical linkages can be used to predict coastal marsh response to SLR and forecast changes in carbon dynamics
- Water efflux and coastal marsh zonation patterns are dynamically linked to terrestrial groundwater table and relative sea-level rise
- Hydrologic setting could impact ability of marshes to migrate landward



This article has been accepted for publication and undergone full peer review but has not been through the copyediting, typesetting, pagination and proofreading process which may lead to differences between this version and the Version of Record. Please cite this article as doi: 10.1029/2019WR026302

**Abstract**

Coastal marshes are an important component of the global carbon cycle, yet our understanding of how these ecosystems will respond to sea-level rise (SLR) is limited. Coastal marsh hydrology varies based on elevation, distance from channel, and hydraulic properties, resulting in zones of unique water level oscillation patterns. These zones impact ecology and geochemistry and correspond to differences in carbon accumulation rates. These physical-biogeochemical linkages enable use of a hydrological model to predict changes in marsh zonation, and in turn carbon accumulation, as well as groundwater-surface water exchange under SLR. Here, we developed a calibrated hydrological model of a Delaware coastal marsh using HydroGeoSphere. We simulated three scenarios each of SLR, sediment accretion, and upland hydrologic response, and we quantified changes in the spatial coverage of different hydrologic zonations and groundwater-surface water exchange. Results show that relative SLR reduces marsh area, carbon burial, and lateral water fluxes. However, the magnitude of changes is linked to terrestrial groundwater table as well as relative SLR. In scenarios where the upland water table does not change with SLR, the magnitude of decline in marsh area and carbon accumulation is reduced compared to scenarios where the upland water table keeps pace with SLR. In contrast, the reduction in lateral water flux is minimized in scenarios with an upland water table rise equal to SLR compared to scenarios where the upland water table is held at present-day levels. This study highlights the importance of regional hydrologic setting in the fate of coastal marsh dynamics.

**Plain Language Summary:**

Coastal marshes are efficient carbon sinks, but their location at the land-sea interface makes them vulnerable to sea-level rise. Through a web of complex interactions, coastal marsh hydrology, which is spatially variable, impacts carbon burial. This link between ecosystem processes enables the use of a physical, hydrological model to forecast changes in hydrology under variable relative sea-level rise scenarios that can be related to alterations in carbon accumulation across the marsh. Our results show that both sea level and the water table on land impact coastal marsh hydrology. Results show a decrease in marsh area and carbon sequestration capacity with sea-level rise, and variations in relative sea-level rise and groundwater table response to climate change impact the magnitude of these effects.

## 1. Introduction:

Coastal marshes have gained widespread attention in recent decades due to both their carbon storage capacity and their uncertain fate in the face of global environmental change. Coastal marshes store more carbon per hectare than terrestrial ecosystems (Mcleod et al., 2011), but their location at the interface between land and sea makes them vulnerable to inundation due to sea-level rise (SLR) (Craft et al, 2009) and deterioration due to the influences of coastal urbanization (Deegan et al., 2012). Despite their importance in the present and future global carbon cycle, the response of coastal marsh carbon dynamics to environmental change is largely unknown, particularly how and how much carbon marshes will capture and store.

One reason for uncertainty in future marsh carbon dynamics is variability in the hydrologic response to environmental change. Coastal marsh hydrology is complex due to diurnal water level oscillations, subsurface heterogeneity, and microtopography (e.g., Sawyer et al., 2016) and dynamically linked to ecology and biogeochemistry. Near tidal channels, water level fluctuations in the creeks create hydraulic gradients that drive water into and out of creek banks (Nuttle, 1988; Wilson & Gardner, 2006; Xin et al., 2011), enabling diurnal sediment aeration and porewater flushing. The tidal zone of influence is governed by tidal amplitude, marsh topography, and permeability of the near-creek sediment (Harvey et al., 1987; Wilson & Morris, 2012; Xin et al., 2013). Additionally, crab bioturbation, concentrated near tidal channels, impacts near-creek hydrology and can increase subsurface-surface water exchange and aeration (Xin et al., 2009; Xiao et al., 2019; Guimond et al., 2019). Away from this dynamic near-creek circulation zone, the marsh interior is influenced by vertical hydraulic gradients induced by elevation-dependent flooding, precipitation, and evapotranspiration (Hemond and Fifield, 1982; Nuttle, 1988; Xin et al., 2013). Lower elevation areas are characterized by nearly persistent, tidally influenced flooding, except during neap tides, and aeration and flushing are limited. In contrast, the hydrology of higher elevation areas is mediated predominantly by spring-neap water level fluctuations and thus characterized by a larger unsaturated zone and periodic flushing.

These unique hydrological zones impact vegetation mosaics and carbon accumulation. Vegetation is influenced by hydrology through variation in soil aeration, inundation frequency, salinity, and porewater flushing, resulting in distinct vegetation zonations across the marsh platform that correspond to hydrologic zones (Moffett et al., 2012; Wilson et al.,

2015a; Xin et al., 2013). Hydrology indirectly impacts carbon accumulation through regulation of vegetation type which impacts carbon accumulation due to differences in belowground productivity (Choi et al., 2001; Elsey-Quirk et al., 2011; Ouyang & Lee, 2014). Additionally, hydrology directly impacts carbon accumulation through influence on soil aeration and microbially mediated carbon oxidation, sediment deposition, and lateral flushing. For example, carbon storage is greater in low and middle marsh areas that experience regular flooding compared to periodically-inundated, high marsh areas (Choi et al., 2001, Elsey-Quirk et al., 2011). Similarly, areas colonized by *Spartina,* a dominant species in low and middle marsh areas, have higher carbon accumulation rates than areas colonized by *Distichlis,* a high marsh species (Ouyang & Lee, 2014). Thus, distributions of vegetation and hydrology, which are linked, impact net ecosystem carbon burial.

Despite the linkages between vegetation and carbon burial, predicting future marsh carbon burial based on vegetation changes is limited to empirically based estimates (Morris et al., 2002; Valiela et al., 2018). However, both vegetation zonations and subsurface redox conditions are linked to subsurface hydrology (Moffett et al., 2012; Wilson et al., 2015a; Bothfeld, 2016; Guimond et al., 2019), which can be simulated using physics-based numerical models that can incorporate changes in space and time. Numerical models of coastal marshes typically focus primarily on surface water and sediment dynamics (Fagherazzi et al., 2012), as these are important processes to the vertical accretion of a marsh and thus marsh survival under SLR. However, these studies frequently overlook subsurface hydrologic processes (i.e. groundwater flow, groundwater-surface water exchange) which are intimately linked to vegetation zonation and carbon sequestration, and therefore also related to marsh persistence in the face of SLR. Hydrological, or ecohydrological, zonations can be distinguished based on water table elevation and oscillation pattern (Wilson et al., 2015a; Xiao et al., 2017; Xin et al., 2013; Guimond et al., 2019) providing a physical-biogeochemical linkage that traditional coastal marsh delineations (i.e. low, mid, high marsh or vegetation species) do not provide and traditional models do not incorporate. Based on this linkage, the proportions of hydrologic zones across an ecosystem can be determined from numerical models and used to assess carbon burial under varied hydrological conditions.

Hydrological modeling can also elucidate the lateral fluxes of water and its constituents to estuaries and continental shelf waters, enhancing present and future budget estimates. The dissolved, lateral transport of carbon from tidal marshes to estuaries and the coastal ocean is a particularly poorly constrained component of coastal carbon budgets, yet

recent work has identified lateral transport as a significant outlet for sequestered carbon (Wang et al. 2016, Najjar et al. 2018, Herrmann et al., 2015, Bauer et al. 2013). Thus, a better understanding of magnitudes and mechanisms of lateral export is of great importance.

The magnitude of carbon exported laterally from coastal marshes is both a function of the quantity of groundwater-surface water exchange and the concentration of dissolved carbon in the exchanged porewater. The magnitude of exchange is proportional to tidal amplitude and inversely related to mean sea level (Harvey et al., 1987, Wilson and Morris, 2012; Wilson et al., 2015b), which suggests that water exchange would decrease with SLR (Wilson et al., 2015b). However, depending on the geologic and hydrologic setting, an increase in mean sea level may also increase the terrestrial water table elevation (Rotzoll & Fletcher, 2013), adding an additional factor to the SLR – lateral exchange relationship.

The linkages between the hydrology and geochemistry discussed above enable the use of a hydrological model to understand changes in coastal marsh hydrodynamics and extrapolate to changes in carbon dynamics due to long-timescale hydrologic perturbations. In this study, we develop a calibrated hydrological model of a mid-Atlantic coastal marsh and use it to simulate three SLR and three sediment accretion scenarios along with three terrestrial head conditions. Specifically, we evaluate how SLR and changes in terrestrial groundwater table impact coastal marsh hydrologic zonations and groundwater-surface water exchange and extrapolate these changes to changes in future carbon dynamics. Results highlight the role of upland groundwater table elevation in mediating coastal marsh response to relative SLR (RSLR) and suggest a tipping point exists at which marsh area and carbon accumulation rapidly decline. This study informs present-day carbon dynamics and will improve prediction of future changes to both coastal marshes and bordering ecosystems with SLR.

## 2. Methods

### 2.1 HydroGeoSphere

A numerical finite-element model was developed using *HydroGeoSphere* due to its ability to simulate a 3-D, variably saturated system and coupled surface and subsurface flow regimes (Therrien et al., 2006). *HydroGeoSphere* uses the diffusion-wave approximation of the Saint Venant equation to simulate 2-D surface water flow plan view, and the Richards equation to calculate the 3-D, variably saturated subsurface flow system (Therrien et al.,

2006). The surface and subsurface domains are coupled using the dual node approach, where the two domains are separated by a thin porous layer with a pre-determined thickness (i.e. coupling length). Darcy's Law is then used to compute the fluid exchange between the two domains. A more in-depth discussion of *HydroGeoSphere*'s theory, governing equations, and numerical solution techniques can be found in Therrien et al. (2006).

**2.2 Model domain, parameters, and boundary conditions.**

The model domain encompasses 2.41 $km^2$ of St. Jones National Estuarine Research Reserve and the surrounding coastal marsh and forest (Figures 1 and 2). The base of the model domain is 12 m below the NAVD88 datum which is the base of the unconfined aquifer as suggested by the Delaware Geological Survey well-log records (He & McKenna, 2014). The surface mesh is unstructured, with finer spacing near tidal channels, and coarser spacing in the middle marsh and forest areas, allowing for balance between simulation speed and mesh resolution (Figure 2). The model grid has 58,410 nodes and 102,320 elements of variable size. To ensure that discretization did not significantly impact our results, one simulation was run with higher discretization and showed only minor differences in head (Text S1, Figure S1). The surface topography was imported from a LiDAR-derived Digital Elevation Model (DEM) created by the Delaware Geological Survey (McKenna et al., 2018). Where possible, a corrected DEM was used which compensated for the vegetation-specific positive elevation bias. Otherwise, a standard 0.25 m correction factor was removed from the DEM elevation to account for the vegetation bias based on assessment of ~75 GPS-RTK measurements within the calibration area. Nodes within tidal channels were manually corrected based on GPS-RTK measurements and a linear interpolation between GPS-RTK points.

There are eight subsurface layers increasing in thickness from the surface to the base of the model (i.e. 0.25 m to 7 m). The base layer is uniformly 7 m thick from -12 m to -5 m. From -5 to -2 m, there are three uniform layers 1 m in thickness. Above -2 m, the four layers vary in thickness based on topographic elevation, ranging from 0.125 m thick at the lowest point in the river to 1.1 m thick at the highest point in the forest. Overland properties were assigned to the surface domain and porous media properties were assigned to 5 units in the groundwater domain (Table 1, Figure 2). The units were based on field data including well logs (He & McKenna, 2014), crab burrow surveys (Guimond et al., 2019), slug tests (Guimond et al., 2019), and soil cores (Bothfeld, 2016). In the porous media domain, the

forest unit, delineated based on well logs (He & McKenna, 2014), visual inspection, and LiDAR imagery, encompassed the top cell (~1 m deep) in terrestrial areas landward of the present-day marsh; the bioturbated marsh unit encompassed the top cell (~0.25 m deep) of areas close to the main tidal channel where heavy bioturbation occurs based on Guimond et al. (2019); the near surface marsh unit ranged from elevations of -0.5 to 1.5 m based on slug tests (Guimond et al., 2019) and soil cores (Bothfeld, 2016), capturing the surface of the marsh in areas other than the bioturbated unit; the deep marsh unit captured -5 m to -0.5 m, encompassing the lower hydraulic conductivity sediment at depth across the entire domain, based on slug tests and well logs (He & McKenna, 2014); and the sandy aquifer unit, -12 m to -5 m, represented the underlying sandy unconfined aquifer as indicated by well logs (He & McKenna, 2014). The bioturbated marsh unit was only included in summer simulations (July-September, 2018) when burrows were more prevalent and had the greatest impact on hydraulic properties (Guimond et al., 2019).

A variable-head boundary condition was assigned to the southwestern edge of the domain – the intersections of the marsh and St. Jones River (AD, Figures 1 and 2). The river level was based on data from the St. Jones River, collected by the National Estuarine Research Reserve (NERR) Monitoring Network (NOAA) (Figure 2). A second variable-head boundary condition was assigned to the upland, terrestrial boundary of the domain (therein referred to as the terrestrial head boundary) with groundwater head based on conductivity-temperature-depth (CTD) data from the unconfined aquifer (BC, Figure 1 and 2). The base and non-river or forested portions of domain edges (AB & DC) were no-flow boundaries. Both evapotranspiration and rainfall were designated as variable flux boundary conditions on the top model-face, rain based on weather station data via NERR Network (NOAA), and potential ET assigned a constant daytime value, magnitude based on literature and refined based on calibration (Table S1, Figure 2). Summer potential ET was 4 mm $d^{-1}$ and 2 mm $d^{-1}$ for fall and winter/spring which are within the range of values in the literature (Table S1).

Simulations were all run as single-density due to the nearly uniform salinity of this saline coastal marsh system. To ensure that the exclusion of variable-density did not significantly impact our results, two-dimensional variable- and single-density models were run and groundwater-surface water exchange was quantified. There was no significant difference in the exchange flux between the single and variable density simulations, and thus all three-dimensional simulations were run without variable density, greatly reducing computation time.

### 2.3 Model calibration and sensitivity analysis

Porous medium and overland flow properties were initially prescribed based on literature values and field data and refined based on calibration. Sensitivity analyses were conducted on saturated and unsaturated properties, including hydraulic conductivity, porosity, and van Genuchten parameters, as well as evapotranspiration and overland flow properties. The range of values for each parameter were appropriate for the coastal marsh and sandy aquifer sediment and based on literature (Table 1 & S1). Analyses showed that groundwater heads were most sensitive to changes in isotropic hydraulic conductivity and Van Genuchten alpha and beta parameters. Model output was least sensitive to changes in porosity and residual saturation. For example, low values of K (i.e. $10^{-5}$ m $d^{-1}$) in the near surface marsh showed almost no tidal response whereas high values of K in the near surface marsh and/or deep marsh resulted in lower heads and more drainage.

After sensitivity analyses were conducted, K, ET, and van Genuchten parameters were manually changed for each parameter unit in order to achieve the best fit across the different hydrologic zones (Table S1; Figures S2). Hydraulic conductivity in the bioturbated marsh and near surface marsh units was varied based on monthly slug test measurements made in monitoring wells within the model domain (Guimond et al., 2019). Hydraulic conductivity in the sandy aquifer was based on slug tests conducted by the Delaware Geological Survey (He & McKenna, 2014). The model was calibrated to water table elevation data collected from CTD loggers deployed in wells located across the marsh platform but confined to an area within the model domain (Figures 1, S2). There are 4 wells in the bioturbated marsh unit, 6 wells in the near surface marsh unit, and 4 wells in the sandy aquifer unit. However, in terms of the hydrologic zones, there are 4 wells in the tidal-near channel, 2 wells in the tidal-interior, 4 wells in the spring-neap, and 4 wells in the upland. While the instrumented area encompasses only a portion of the model domain (Figure 1), the wells are located in different units, vegetation zonations, and distances from the channel such that the hydrologic signals measured represent the different settings within the larger marsh area. Although we were unable to access other areas of the marsh for instrumentation, we believe that these locations are representative of the marsh within the model area, as well as mid-Atlantic brackish marshes in general. Calibration simulations were run for July 2017 and March-April 2018 and compared to water table elevation data collected from 7-10 wells over

the same time period. The calibration time periods, representing one quarter of a year, were chosen based on maximum data availability and computational time and are representative of periods with and without bioturbation. Additional comparisons were made between field and model data for October-November, 2017 (Figure S3) to ensure the model adequately represented time periods outside the calibration period.

Model results capture the hydrologic patterns and characteristics that distinguish each hydrologic zone (Figure S2 and S3) (Guimond et al., 2019). Hydrologic zones were based on water table elevation data collected across the marsh platform. Analysis revealed distinct hydrologic zones that differed by fluctuation frequency and average depth to water table (Guimond et al., 2019). Within the marsh, the tidal-near channel zone had large diurnal water table elevation fluctuations that varied with the tidal channel; the spring-neap zone had longer timescale fluctuations (spring-neap) and encompassed higher elevation areas; and the tidal-interior zone showed tidal and spring-neap fluctuations close to or above the marsh surface. While these zones roughly correspond to those proposed by Wilson et al. (2015a) and Xin et al. (2013), the zones are named based on their hydrological characteristics. Additionally, the subtidal zone was always inundated, and the upland zone, landward of the marsh, exhibited longer timescale fluctuations and a deeper unsaturated zone. Discrepancies between measured and simulated head arise from several factors, including: 1) errors in the DEM, 2) spatial offset in observations and simulation location due to node resolution, and 3) assumption of constant evaporation rate that does not account for inter-daily variation or vegetation-specific changes in evapotranspiration. The greatest error can likely be attributed to the DEM. While we used the most up-to-date DEM of our study region and made corrections based on site-specific data, saltmarshes are inherently challenging to image due to the dense vegetation, surficial flooding, and microtopography.

**2.4 Simulations**

Simulations covered three distinct time periods: 1) October-November 2017, 2) February-March 2018, and 3) July-September 2018, capturing the fall, winter/spring, and summer seasons. July-September 2018 incorporated increased tidal-near channel K (bioturbated marsh unit). In the summer, marsh crabs bioturbate the marsh, predominantly near the tidal channel (Katz, 1980). Bioturbation increases K and groundwater-surface water exchange (Guimond et al, 2019; Xiao et al., 2019; Xin et al., 2009). Model results (i.e. fluxes and zonations) from each time period were extrapolated to represent each seasonal period and

averaged to arrive at an annual value (see Text S2 and Text S3 for more information on seasonal extrapolation). Initial heads were started from steady-state conditions which use the average terrestrial head and average river head boundary conditions for the season and sea-level scenario.

For each time period, 10 simulations were completed including a present-day simulation and nine additional simulations with relative sea-level rise (RSLR) ranging from -0.08 m to 1.33 m (Figure S4). RSLR scenarios were based on three SLR scenarios for the year 2100 (0.5 m, 1.0 m, and 1.5 m) (Callahan et al., 2017), and three sediment accretion scenarios based on low, moderate, and high sediment accretion rates (0.17, 0.41, and 0.58 m) (Siok, 2017). It is important to note that the mid-Atlantic United States has some of the highest SLR rates in the world due to land subsidence. Additionally, for each time period, each of the 9 simulations were run three times with different terrestrial heads (Figure S4): 1) terrestrial head remained the same as present-day, 2) terrestrial head increased 54% of SLR (Knott et al., 2019), and 3) terrestrial head increased equivalent to SLR. A total of 84 simulations were run.

### 2.5 Quantification of groundwater-surface water exchange

The magnitude of water exchanged between the surface and subsurface domains was calculated using the dual node approach and Darcy's Law:

$$q = K \cdot k_r \nabla(\psi + z)$$

where $q$ is the exchange flux, $K$ is the hydraulic conductivity tensor, $k_r$ is the relative hydraulic conductivity, $\psi$ is the pressure head, and z is the elevation head (Therrien et al., 2006). Positive flux indicates water entering the surface domain from the subsurface. To quantify the groundwater-surface water exchange within tidal channels in the model domain, nodes within all tidal channels were isolated. Within the isolated domain, the node flux of each element vertex (3 nodes) was averaged and multiplied by the element area to get the volumetric discharge for each surface element. The sum of the volumetric discharge for all elements within the channel for the simulation time divided by the total simulation time was the total daily discharge ($m^3/d$).

### 2.6 Hydrologic zone and carbon assessment criteria

To determine the spatial distribution of each hydrologic zone, each node within a subset of the model domain (Figure 1) was treated as an observation well which enabled

output of the hydraulic head with time. Observation wells were all placed 0.5 m below the domain surface.

The hydraulic head of each node was processed for the magnitude of dominant tidal signals using a Fast-Fourier Transform (FFT), the percent of time inundated (i.e. hydroperiod), and the average head. The hydrologic zone criterium (Table 2) was established based on analysis of water table elevation data from monitoring wells within the model domain (Figure 1). The tidal signal and hydroperiod of each well were analyzed and revealed three zones that differed based on the magnitude of the principal lunar tidal signal (M2), the magnitude of the long-duration tidal harmonics, and hydroperiod. The hydraulic head output for each zone was used to categorize each node into a hydrologic zone. Whereas similar zones are present in other marsh literature and defined using alternative indices (e.g. Xin et al., 2013, Moffett et al., 2010, Wilson et al., 2015a), the criterion used in this study enables use of a hydrogeological model to predict future hydrologic conditions.

To calculate the total carbon accumulation for the model domain, we assigned each hydrologic zone a range of carbon accumulation rates based on literature values. As designation of the hydrologic zone incorporates consideration of unsaturated depth and duration, which is a major control on carbon respiration rates (e.g., Guimond et al., 2019), assignment of zone-specific carbon accumulation rates captures spatial variability. The maximum and minimum rate for each zone (Table 2) was based on literature values for Delaware marshes (Tucker, 2016), high and low marsh (Choi & Wang, 2004), and vegetation type (Ouyang & Lee, 2014; Schlesinger, 1997). The range accounts for the high variability in carbon accumulation rates. For total carbon accumulation, we multiplied the area of each hydrologic zone by the maximum and minimum rate for each zone.

## 3. Results

### 3.1 Hydrologic zonations

The spatial distribution of hydrologic zones (i.e. subtidal, tidal-near channel, spring-neap, tidal-interior, and upland) varied with RSLR and the terrestrial head response to SLR (Figures 3 and 4). In general, as RSLR increased, the subtidal area increased, the upland area decreased, and the total marsh area (tidal-near creek, spring-neap, and tidal-interior) decreased (Figures 3-5). However, deviations from these generalized trends existed. Under RSLR between 0.09 – 0.42 m, the marsh area expanded for all terrestrial head boundary scenarios as marsh hydraulic signals propagated into the upland and large conversion to

subtidal zone had not yet occurred (Figure 5). Total marsh area decreased for RSLR above 0.42 m when the terrestrial head boundary was equal to present-day or increased 54% of SLR because lower terrestrial water levels minimized landward migration of marsh zones. When the terrestrial head boundary increased equivalent to SLR, the marsh area remained larger than present-day until 0.83 m RLSR when it was nearly equal to present-day and after which the area rapidly decreased (Figure 4). The higher terrestrial head boundary increased the water table elevation such that marsh hydrologic signals were able to migrate further landward with RSLR. However, there was a threshold at which the higher water table was no longer beneficial to marsh area. Above 0.83 m, when the terrestrial head boundary increased equivalent to SLR, the marsh area was 0.076-0.115 $km^2$ smaller than other terrestrial head scenarios due to enhanced conversion to subtidal zone (Figures 4 and 5).

The terrestrial head response to SLR also determined what hydrologic zone migrated into the present-day upland zone (Figures 3 and 4). During periods of marsh expansion (i.e. RSLR $\leq$ 0.42 m), when the terrestrial head was held to the current level, the increase in total marsh area occurred due to an increase in spring-neap zone area at the expense of the upland zone area. Conversely, when the terrestrial head increased with SLR, the increase in marsh area occurred due to an increase in the tidal-interior zone at the expense of the upland zone (Figure 3). This is because the water table was located closer to the ground surface for increased terrestrial head simulations compared to simulations with no terrestrial head response to SLR. Above 0.42 m RSLR, under present-day terrestrial head scenarios, the tidal-near channel zone area increased and the tidal-interior zone area remained constant. When the terrestrial head increased with SLR, the tidal-near creek area remained low and constant and the tidal-interior zone area increased up to 0.83 m RLSR, and then decreased. Terrestrial head had a greater impact on the area of the tidal-interior zone when compared to an equal rise in sea level, but RLSR has a greater impact on area of the other hydrologic zones. Again, this points to the terrestrial head impacting marsh water level and in turn hydrologic zonation. Scenarios with an increase in terrestrial head 54% of SLR were intermediate between the other two terrestrial head scenarios.

### 3.2 Hydrologic zone carbon assessment

Similar to hydrologic zones, the projected total carbon burial was dependent on RSLR and terrestrial head conditions (Figure 6). Under high SLR scenarios (1.5 m, RSLR $\geq$ 0.93 m), the net carbon accumulation decreased for both high and low carbon accumulation rate

ranges and all terrestrial head scenarios (Figure 6). However, below 0.59 m RSLR, carbon accumulation exceeded that of present-day due to marsh expansion. In general, carbon accumulation was greater when terrestrial head increased equivalent to SLR due to an increase in zones with high carbon accumulation rates (tidal-interior) (Figure 6). However, for high RSLR scenarios (≥ 0.93 m), carbon accumulation was greater when terrestrial head was held at present-day levels with SLR.

### 3.3 Lateral Water fluxes

The total exchange of groundwater from the marsh platform to tidal channels was impacted by both relative sea level and the terrestrial boundary head (Figure 7). In general, groundwater-surface water exchange decreased with SLR but, within each SLR scenario, exchange was higher under elevated sediment accretion scenarios because RSLR was lower (Figure 7). When the terrestrial head was kept at present-day levels with SLR, the total exchange flux into tidal channels decreased for all positive RSLR scenarios, decreasing from 1807 $m^3/d$ present-day to 244 $m^3/d$ under 1.33 m RSLR. However, when an increase in the terrestrial head was included, hydraulic gradients were maintained and the decrease in exchange with RSLR was minimized. The exchange flux decreased from 1807 $m^3/d$ to 636 $m^3/d$ and 1807 $m^3/d$ to 1030 m3/d for an increase in terrestrial head 54% and 100% of SLR, respectively. Similar patterns held when assessing the per meter tidal channel flux in a section of the main tidal channel dissecting the model domain. The present-day flux per meter of tidal channel was 0.46 $m^3/d$ and decreased to 0.02 $m^3/d$ per m tidal channel and 0.15 $m^3/d$ per m tidal channel for an increase in terrestrial head 0% and 100% of SLR, respectively.

The highest marsh platform to tidal channel fluxes occurred in the spring and to a lesser extent summer, and the lowest fluxes occurred in the fall. This is likely due to higher average upland groundwater table elevations in the winter/spring than the fall, increasing the hydraulic gradient and groundwater flow toward the marsh.

## 4. Discussion

This study demonstrates how a hydrological model and our understanding of coupled hydro-biogeochemical processes can be used to predict coastal marsh response to SLR and forecast changes in coastal carbon dynamics. Our general projections of hydrological (and associated vegetation) mosaics and carbon burial are similar to previous studies based on empirical (Valiela et al., 2018) and surface-based models (Kirwan & Mudd, 2012). However,

the physics-based model was able to provide additional insight into the factors mediating these trends as well as quantification of water exchange and estimates of future water and carbon fluxes.

### 4.1 Terrestrial head controls on system response

#### 4.1.1 Terrestrial head impacts marsh zonation

Coastal marshes, and thus their carbon storage potential, persist in the face of SLR by vertically accreting through sediment deposition and organic matter accretion (Reed, 1995), or by migrating laterally into terrestrial ecosystems on the landward boundary (Brinson et al., 1995; Kirwan et al., 2016). The potential survival of coastal marshes in the face of SLR is dependent on sediment delivery (Kirwan et al., 2010) and accommodation space, or the necessary space and conditions for marshes to migrate landward (Thorne et al., 2018; Enwright et al., 2016). Our results highlight an important factor that mediates the necessary conditions for lateral marsh migration: terrestrial head.

Marshes are characterized by their shallow groundwater table and frequently saturated conditions. Therefore, in order for marshes to migrate inland, the water table must be near the ground surface and salinity high enough such that marsh plant species can outcompete non-marsh species. Our results show more extensive conversion of upland to marsh with higher terrestrial groundwater tables (terrestrial head increase equal to SLR) compared to when the groundwater table remains far from the marsh surface (terrestrial head remains at present-day levels with SLR). In scenarios with no terrestrial head response to SLR, the upland zone area decreased from 39% to 11% of total domain area (Figure 3). However, in scenarios with terrestrial head response equal to SLR, upland zone area decreased from 39% to 3% of the total domain. The higher groundwater table, combined with a higher seaward boundary, creates a greater area of "marsh like" hydrologic conditions compared to scenarios with a lower groundwater table.

Terrestrial head also impacts changes in inter-marsh hydrologic zone distribution with RSLR. For example, under conservative rates of RSLR (< 0.59 m), when the terrestrial head was held at present-day levels, the spring-neap zone area increased as the upland zone area decreased. Conversely, when terrestrial head increased with SLR, the tidal-interior zone area increased as the upland zone area decreased. The spring-neap zone is characterized by infrequent (lunar) inundation and an overall lower water table with respect to the marsh surface. The tidal-interior is frequently saturated and tidally inundated. Thus, it is a

reasonable prediction that in scenarios with a lower groundwater table, the spring-neap zone migrates landward, and in scenarios with a higher groundwater table, the tidal-interior zone expands.

#### 4.1.2 Terrestrial head impacts lateral exchange

The terrestrial groundwater table elevation also impacts the lateral efflux of coastal marsh porewater and its constituents to estuaries and the coastal ocean. We show that the magnitude of lateral water discharge is regulated by the hydraulic gradient between the marsh and upland, a balance between RSLR and terrestrial head (Figure 7). Steeper hydraulic gradients (i.e. greater terrestrial head response to SLR and lower RSLR) increased groundwater flow toward the lower-head tidal channel, enhancing lateral efflux. As RLSR increased and/or the terrestrial head remained at present-day levels, hydraulic gradients decreased, minimizing seaward groundwater flow.

The role of hydraulic gradients in lateral water efflux also impacts the total amount of carbon stored in coastal marshes. Greater exchange and flushing under increased hydraulic gradients decrease the amount of carbon trapped in the marsh platform and potentially increase respiration rates through introduction of oxygen-rich water to the subsurface (Guimond et al., 2019; Bothfeld, 2016). Our results show that under most RSLR scenarios the lateral water exchange decreased with RSLR, the magnitude of decrease ranging from 22 $m^3/d$ to 1564 $m^3/d$, suggesting a decrease in carbon delivery to bordering ecosystems (i.e. estuaries or coastal ocean) and an increase in the amount of carbon stored in the marsh platform. However, under some scenarios, the lateral exchange from the marsh platform to tidal channel increased, as much as 550 $m^3/d$, suggesting that when hydraulic gradients between the land and sea are maintained or increased via enhanced recharge, the magnitude of carbon lost from coastal marshes could be greater than or equal to present-day.

#### 4.1.3 Conceptualization with respect to coastal hydrologic setting

The relationship between water/carbon exchange and hydraulic gradients enables changes in exchange to be conceptualized in terms of the coastal hydrologic setting (Michael et al., 2013). Coastal groundwater systems can be divided into two types: topography-limited and recharge-limited. In topography limited systems, the groundwater table is close to the ground surface such that the water table cannot rise in response to hydrologic change such as SLR. In these systems, an increase in head causes the groundwater table to intersect the land surface, activating new surface discharge locations and maintaining the same head, thus the land-sea

hydraulic gradient would decrease with SLR. Conversely, in recharge-limited systems, the groundwater table is far beneath the land surface such that an increase in groundwater-table elevation does not intersect the land surface and the land-sea hydraulic gradient is maintained with SLR (Haitjema and Mitchell-Bruker, 2005; Gleeson et al., 2011; Michael et al., 2013). The control of the hydraulic gradient on groundwater-surface water exchange suggests that topography-limited systems will experience a greater decline in lateral carbon export compared to recharge-limited systems.

Similarly, the impact of water table on marsh migration enables conceptualization in terms of hydrologic setting. Successful migration is most probable in topography-limited systems where the groundwater table is close to the land surface compared to recharge-limited systems where the water table is too far from the land surface to create marsh-like conditions as the water table rises in response to SLR. This conceptualization aligns with previous studies where a steep slope (likely found in a recharge-limited area such as parts of the west coast) inhibits lateral marsh migration (Thorne et al., 2018; Smith, 2013). As a result, a map of most probable marsh migration regions could follow the Michael et al. (2013) map of topography- and recharge-limited coastlines, where one would expect topography-limited coastlines to have more ideal conditions for marsh migration.

### 4.2 Implications of zone shifts on carbon cycling

If there is accommodation space and the required conditions for marshes to migrate, carbon accumulation in marshes could remain constant or increase under conservative RSLR scenarios (Figure 6). However, in many places, human development and hardening of coastlines limit lateral migration (Gittman et al., 2015; Thorne et al., 2018). In the United States alone, approximately 14% of the coastline is armored (Gittman et al., 2015). Many agricultural fields, especially in the mid-Atlantic, lie within 1 km of a coastal marsh, and actions by farmers to minimize loses to their cropland effectively create anthropogenic barriers to marsh migration.

Allowing marsh migration into upland, our analysis shows a decrease in carbon burial above 0.42 m RSLR (Figure 6). If we did not enable upland conversion to marsh, a decrease in marsh area and carbon storage may occur even more abruptly (Figure S9). This highlights the importance of land conservation landward of marshes, as the loss of marsh creates a positive feedback with the global carbon cycle. With less carbon sequestered by coastal

marshes, more carbon remains in the atmosphere, fueling increasing atmospheric $CO_2$ concentrations and global climate change, further increasing SLR and marsh drowning.

### 4.3 Ecological Implications

Intra-marsh variation in the zone distribution with RSLR has important implications for rare bird species that inhabit marshes. The saltmarsh sparrow (*Ammodramus caudacutus*) lays its eggs in high marsh (i.e. spring-neap zone) areas (DiQuinzio et al., 2006; Gjerdrum et al., 2005). Already, more frequent inundation of the marsh platform and diminishing high marsh areas is causing a rapid decline in these species' populations (Gjerdrum et al., 2005; Berry et al., 2015). Complete elimination of high marsh suggests a grim outlook for the saltmarsh sparrow, and other bird species such as the black rail (*Laterallus jamaicensis*) that rely on high marsh to live and raise their young. However, under some conditions, high marsh may expand (i.e. hydrologic settings where groundwater table does not respond to SLR and RSLR is less than 0.83 m), keeping important habitat necessary for the survival of these species.

Additionally, varied hydrological conditions may impact the distribution and abundance of crab burrows which have been shown to impact marsh porewater flow and biogeochemistry (Xin et al., 2009; Fanjul et a., 2011; Montague, 1982). Burrows act as conduits for preferential water flow that increase sediment permeability (Gingras et al., 1999; Guimond et al., 2019), groundwater-surface water exchange (Stahl et al., 2014; Xin et al., 2009; Xiao et al., 2019), and variability in soil saturation (Xiao et al., 2019). These hydrological changes impact marsh biogeochemistry through changes in plant productivity, porewater salinity, and oxygen penetration into the sediment. Furthermore, changes in burrow distribution and abundance have the potential to impact the carbon budget of coastal marshes through changes in the magnitude of carbon oxidation and lateral carbon transport. Crab burrows are most prevalent near tidal channels (Wasson et al., 2019; Katz, 1980; McCraith et al., 2003; Teal, 1958). An increase in the tidal-near creek zone area could increase crab burrow populations, whereas an increase in the tidal-interior, where few crabs inhabit, may decrease the number of burrows, impacting groundwater flow and biogeochemistry.

Changes in the lateral export of water and carbon have implications beyond the bounds of the marsh itself. The nutrients and organic matter exported from coastal marshes are hypothesized to fuel high primary productivity in connected estuarine ecosystems (Odum, 1980), and thus, this coastal marsh-originated food source is important to estuarine consumers such as fish and bivalves. A decrease in the exchange and lateral export of water

and its constituents from coastal marshes to estuaries suggests a decrease in nutrient and organic matter delivery to estuarine fish and invertebrate species. However, organic carbon export not only fuels high estuarine productivity, but it is also hypothesized to fuel coastal ocean net heterotrophy and estuarine carbon dioxide ($CO_2$) degassing (Cai, 2011). Thus, a decrease in the lateral carbon export from coastal marshes may impact the autotroph/heterotroph balance of the coastal ocean and the efflux of $CO_2$ from estuaries. Conversely, this lateral export of water, and with it dissolved inorganic carbon and alkalinity, has also been suggested to increase the buffering capacity of the coastal ocean (Wang et al., 2016). Therefore, a decrease in lateral exchange may impact the coastal ocean's resistance to ocean acidification. A more thorough assessment of porewater biogeochemistry is necessary to more fully understand the effects of lateral carbon export.

### 4.4 Uncertainty and Future Research

There are a number of uncertainties to consider in this study beyond those stated above. For example, the zonation projections assume that lateral migration can occur. However, it is known that numerous ecological shifts must happen before a marsh can migrate into upland forest, including thinning of the forest canopy, decline in regrowth, and eventually death of tree species through impacts of storm surge and salinization (Fagherazzi et al., 2019), as well as elimination of human barriers. When migration cannot occur, either due to anthropogenic or ecological barriers, total marsh area will experience coastal squeeze, with physical or ecological barriers on one boundary and SLR on the other. Whereas the terrestrial head response to SLR may contribute to the viability or efficacy of lateral migration, preservation of land for migration is necessary under all terrestrial conditions in order for marsh area to have a chance of persisting where sedimentation is limited or SLR rates are high.

An additional limitation of this study is the exclusion of salinity. While this simplification did not affect the results of this study focused on the hydrologic system (see Methods), salinity and saltwater intrusion are important factors for vegetation species colonization, marsh platform biogeochemistry, and marsh migration. Future studies that include simulation of salt transport, along with groundwater table elevation and oscillation pattern, will provide insight to the timing of upland forest death and help determine the species able to migrate laterally.

Variability in carbon accumulation rates is an additional source of uncertainty in our carbon accumulation calculation. Even incorporating a range of carbon accumulation rates (high and low) may not capture the specific carbon accumulation rate for each zone or present and future variations within each zone. For example, the magnitude and composition (i.e. mineral vs organic) of material contributing to sediment accretion and carbon accumulation is spatially and temporally variable (i.e. estuarine marsh, riverine marsh) and will contribute to variations in present and future carbon sequestration (Mudd et al., 2009; Elsey-Quirk et al., 2011). For the purpose of this analysis, carbon burial rates used for the calculation were consistent across all RSLR scenarios and did not account for changes in sediment deposition or composition in space or time. However, our analyses and range of carbon accumulation values (Table 2) captures trends in carbon accumulation and how it varies with RSLR and upland groundwater table elevation.

Lastly, soil building, sediment transport, and erosion processes were not considered in this study, yet they are important components of coastal ecosystems and carbon budgets. The timing of the soil building processes in terms of lateral marsh migration is just starting to be explored, thus carbon sequestration in newly developing marshes is not well understood. In this study, the hydrologic pattern determines the carbon accumulation rate, which neglects the timing of transition zones and soil building in the upland boundary. Thus, our analysis may overestimate carbon burial in converted upland areas in the near-term. Furthermore, sediment accretion is not uniform across the marsh surface as we have assumed in this model. The incorporation of sediment dynamics may enhance or diminish coastal marsh area through erosion at the marsh edge or accelerated accretion on the marsh surface. As we look to future development of coastal marsh models, it will be important to couple fully integrated groundwater-surface water models with sediment dynamics models as well as biogeochemical and vegetation models.

## 5. Conclusion

This study uses linkages between coastal marsh hydrology, ecology, and biogeochemistry to enable the use of a hydrological model to enhance our understanding of how coastal marsh functioning and associated carbon dynamics may change in the face of SLR. By using a calibrated hydrological model of a Mid-Atlantic coastal marsh and simulating multiple RSLR and terrestrial head scenarios, we were able to show that projected hydrologic zonations, and

in turn carbon sequestration, as well as lateral exchange of water and carbon, not only depend on RLSR but also on the hydrologic setting that affects terrestrial groundwater heads. Based on hydrologic zone shifts and conversion of marsh to subtidal zone, results suggest marsh area and carbon sequestration may drastically decrease under high RSLR scenarios. Conversely, the exchange flux and lateral carbon export may decrease with RSLR. The changes in marsh zone distribution and carbon sequestration and exchange have implications beyond coastal marshes. Changes will impact productivity in neighboring estuaries, carbon dioxide concentrations in the atmosphere, and sustainability of upland ecosystems.

**Acknowledgements:**

We would like to thank Tom McKenna and the Delaware Geological Survey for access to their monitoring wells. We also thank Xiaolong Geng for his input on model output analyses. This work was supported by the National Science Foundation EAR-1759879. Data is published with CUAHSI Hydroshare (Guimond, 2020).

## 6. References

Bauer, J. E., Cai, W. -J., Raymond, P. A., Bianchi, T. S., Hopkinson, C. S., & Regnier, P. A. G. (2013). The changing carbon cycle of the coastal ocean. *Nature*, *504*(7478), 61–70. https://doi.org/10.1038/nature12857

Berry, W. J., Reinert, S. E., Gallagher, M. E., Lussier, S. M., & Walsh, E. (2015). Population Status of the Seaside Sparrow in Rhode Island: A 25-Year Assessment. *Northeastern Naturalist*, *22*(4), 658–671. https://doi.org/10.1656/045.022.0403

Bothfeld, F. (2016). Spatial and temporal heterogeneity of methane and carbon dioxide production and flux in a temperate tidal salt marsh. MS Thesis, University of Delaware.

Brinson, M. M., Christian, R. R., & Blum, L. K. (1995). Multiple States in the Sea-Level Induced Transition from Terrestrial Forest to Estuary. *Estuaries*, *18*(4), 648. https://doi.org/10.2307/1352383

Cai, W.-J. (2011). Estuarine and Coastal Ocean Carbon Paradox: $CO_2$ Sinks or Sites of Terrestrial Carbon Incineration? *Annual Review of Marine Science*, *3*(1), 123–145. https://doi.org/10.1146/annurev-marine-120709-142723

Callahan, J. A., Horton, B. P., Nikitina, D. L., Sommerfield, C. K., McKenna, T. E., & Swallow, D. (2017). Recommendation of Sea-Level Rise Planning Scenarios for Delaware: Technical Report, prepared for Delaware Department of Natural Resources and Environmental Control (DNREC) Delaware Coastal Programs. 115 pp.

Choi, Y., Hsieh, Y., & Wang, Y. (2001). Vegetation succession and carbon sequestration in a coastal wetland in northwest Florida ' Evidence from carbon isotopes. *Global Biogeochemical Cycles*, 15(2), 311–319.

Choi, Y., & Wang, Y. (2004). Dynamics of carbon sequestration in a coastal wetland using radiocarbon measurements. *Global Biogeochemical Cycles*, *18*(4), 1–12. https://doi.org/10.1029/2004GB002261

Craft, C., Clough, J., Ehman, J., Jove, S., Park, R., Pennings, S., et al. (2009). Forecasting the effects of accelerated sea-level rise on tidal marsh ecosystem services. *Frontiers in Ecology and the Environment*, *7*(2), 73–78. https://doi.org/10.1890/070219

Deegan, L. A., Johnson, D. S., Warren, R. S., Peterson, B. J., Fleeger, J. W., Fagherazzi, S., & Wollheim, W. M. (2012). Coastal eutrophication as a driver of salt marsh loss. *Nature*, *490*(7420), 388–392. https://doi.org/10.1038/nature11533

DiQuinzio, D. A., Paton, P. W. C., & Eddleman, W. R. (2006). Nesting ecology of Saltmarsh Sharp-tailed Sparrows in a tidally restricted salt marsh. *Wetlands*, *22*(1), 179–185. https://doi.org/10.1672/0277-5212(2002)022[0179:neosst]2.0.co;2

Elsey-Quirk, T., Seliskar, D. M., Sommerfield, C. K., & Gallagher, J. L. (2011). Salt marsh carbon pool distribution in a mid-Atlantic Lagoon, USA: Sea level rise implications. *Wetlands*, *31*(1), 87–99. https://doi.org/10.1007/s13157-010-0139-2

Enwright, N. M., Griffith, K. T., & Osland, M. J. (2016). Barriers to and opportunities for landward migration of coastal wetlands with sea-level rise. *Frontiers in Ecology and the Environment*, *14*(6), 307–316. https://doi.org/10.1002/fee.1282

Fagherazzi, S., Anisfeld, S. C., Blum, L. K., Long, E. V., Feagin, R. A., Fernandes, A., et al. (2019). Sea Level Rise and the Dynamics of the Marsh-Upland Boundary. *Frontiers in Environmental Science*, *7*(February), 1–18. https://doi.org/10.3389/fenvs.2019.00025

Fagherazzi, S., Kirwan, M. L., Mudd, S. M., Guntenspergen, G. R., Temmerman, S., Rybczyk, J. M., et al. (2012). Numerical models of salt marsh evolution: Ecological, geormorphic, and climatic factors. *Review of Geophysics*, 50(2011), 1–28. https://doi.org/10.1029/2011RG000359.

Fanjul, E., Bazterrica, M. C., Escapa, M., Grela, M. A., & Iribarne, O. (2011). Impact of crab bioturbation on benthic flux and nitrogen dynamics of Southwest Atlantic intertidal marshes and mudflats. *Estuarine, Coastal and Shelf Science*, 92(4), 629–638. https://doi.org/10.1016/j.ecss.2011.03.002

Gardner, L. R., & Reeves, H. W. (2002). Spatial patterns in soil water fluxes along a forest-marsh transect in the southeastern United States. Aquatic Sciences, 64(2), 141–155. https://doi.org/10.1007/s00027-002-8062-0

Gingras, M. K., Pemberton, S. G., Mendoza, C. A., & Henk, F. (1999). Assessing the anisotropic permeability of Glossifungites surfaces. *Petroleum Geoscience*, 5(4), 349–357. https://doi.org/10.1144/petgeo.5.4.349

Gittman, R. K., Fodrie, F. J., Popowich, A. M., Keller, D. A., Bruno, J. F., Currin, C. A. et al. (2015). Engineering away our natural defenses: An analysis of shoreline hardening in the US. *Frontiers in Ecology and the Environment*, *13*(6), 301–307. https://doi.org/10.1890/150065

Gjerdrum, C., Elphick, C. S., & Rubega, M. (2006). Nest Site Selection and Nesting Success in Saltmarsh Breeding Sparrows: the Importance of Nest Habitat, Timing, and Study Site Differences. *The Condor*, *107*(4), 849. https://doi.org/10.1650/7723.1

Gleeson, T., Marklund, L., Smith, L., & Manning, A. H. (2011). Classifying the water table at regional to continental scales. *Geophysical Research Letters*, *38*(5), 1–6. https://doi.org/10.1029/2010GL046427

Guimond, J. (2020). St. Jones Monitoring Well Data 2017-2018, *HydroShare*, https://doi.org/10.4211/hs.e9de2725c1d442e1bd2ab8e0c4d45efc.

Guimond, J. A., Seyfferth, A. L., Moffett, K. B., Michael, H. A., (2019). A physical-biogeochemical mechanism for positive feedback between marsh crabs and carbon efflux. *Environmental Research Letters.*

Haitjema, H. M., & Mitchell-Bruker, S. (2005). Are water tables a subdued replica of the topography? *Ground Water*, *43*(6), 781–786. https://doi.org/10.1111/j.1745-6584.2005.00090.x

Harvey, J. W., Germann, P. F., & Odum, W. E. (1987). Geomorphological control of subsurface hydrology in the creekbank zone of tidal marshes. *Estuarine, Coastal and Shelf Science*, *25*(6), 677–691. https://doi.org/10.1016/0272-7714(87)90015-1

He, C. and T. E. McKenna. (2014). Using Numerical Models to Evaluate Impacts of Sea Level Rise on Groundwater Resources in the Delaware Coastal Plain, September 2014, Report submitted by the Delaware Geological Survey to the Delaware National Estuarine Research Reserve, 49 p. Delaware Geological Survey, Geophysical log database, www.dgs.udel.edu.

Hemond, H. F., & Fifield, J. L. (1982). Subsurface Flow in Salt Marsh Peat: A Model and Field Study. *Limnology and Oceanography*, 27(1), 126–136.

Herrmann, M., Najjar, R. G., Michael, K. W., Alexander, R. B., Boyer, E. W., Cai, W., et al. (2015). Net ecosystem production and organic carbon balance of U.S. East Coast estuaries: A synthesis approach. *Global Biogeochemical Cycles*, *29*, 96–111. https://doi.org/10.1002/2013GB004736.Received

Hughes, C. E., Binning, P., & Willgoose, G. R. (1998). Characterisation of the hydrology of an estuarine wetland. Journal of Hydrology, 211(1–4), 34–49. https://doi.org/10.1016/S0022-1694(98)00194-2

Katz, L. C. (1980). Effects of burrowing by the fiddler crab, Uca pugnax (Smith). *Estuarine and Coastal Marine Science*, 11(2), 233–237. https://doi.org/10.1016/S0302-3524(80)80043-0

Kirwan, M. L., Guntenspergen, G. R., D'Alpaos, A., Morris, J. T., Mudd, S. M., & Temmerman, S. (2010). Limits on the adaptability of coastal marshes to rising sea level. *Geophysical Research Letters*, *37*(23), 1–5. https://doi.org/10.1029/2010GL045489

Kirwan, M. L., & Mudd, S. M. (2012). Response of salt-marsh carbon accumulation to climate change. *Nature*, *489*(7417), 550–3. https://doi.org/10.1038/nature11440

Kirwan, M. L., Walters, D. C., Reay, W. G., & Carr, J. A. (2016). Sea level driven marsh expansion in a coupled model of marsh erosion and migration. *Geophysical Research Letters*, (43), 4366–4373. https://doi.org/10.1002/2016GL068507.

Knott, J. F., Jacobs, J. M., Daniel, J. S., & Kirshen, P. (2019). Modeling Groundwater Rise Caused by Sea-Level Rise in Coastal New Hampshire. *Journal of Coastal Research*, *35*(1), 143. https://doi.org/10.2112/jcoastres-d-17-00153.1

Loheide, S. P., Butler, J. J., & Gorelick, S. M. (2005). Estimation of groundwater consumption by phreatophytes using diurnal water table fluctuations: A saturated-unsaturated flow assessment. *Water Resources Research*, 41(7), 1–14. https://doi.org/10.1029/2005WR003942

McCraith, B. J., Gardner, L. R., Wethey, D. S., & Moore, W. S. (2003). The effect of fiddler crab burrowing on sediment mixing and radionuclide profiles along a topographic gradient in a southeastern salt marsh. *Journal of Marine Research*, 61(3), 359–390. https://doi.org/10.1357/002224003322201232

McKenna, T. E., Callahan, J. A., Medlock, C. L., Bate, N. S., (2018). *Creation of improved accuracy LiDAR-based digital elevation models for the St. Jones River and Blackbird Creek watersheds*. Newark, Delaware: Delaware Geological Survey

Mcleod, E., Chmura, G. L., Bouillon, S., Salm, R., Björk, M., Duarte, C. M., et al. (2011). A blueprint for blue carbon: toward an improved understanding of the role of vegetated coastal habitats in sequestering CO 2. *Frontiers in Ecology and the Environment*, *9*(10), 552–560. https://doi.org/10.1890/110004

Michael, H. A., Russoniello, C. J., & Byron, L. A. (2013). Global assessment of vulnerability to sea-level rise in topography-limited and recharge-limited coastal groundwater systems. *Water Resources Research*, 49(4), 2228–2240. https://doi.org/10.1002/wrcr.20213

Moffett, K. B., Gorelick, S. M., McLaren, R. G., & Sudicky, E. A. (2012). Salt marsh ecohydrological zonation due to heterogeneous vegetation-groundwater-surface water interactions. *Water Resources Research*, *48*(2). https://doi.org/10.1029/2011WR010874

Moffett, K. B., Robinson, D. A., & Gorelick, S. M. (2010). Relationship of Salt Marsh Vegetation Zonation to Spatial Patterns in Soil Moisture, Salinity, and Topography. *Ecosystems*, 13(8), 1287–1302. https://doi.org/10.1007/s10021-010-9385-7

Montague, C. L. (1982). The influence of fiddler crab burrows and burrowing on metabolic processes in salt marsh sediments. In Estuarine Comparisons (pp. 283–301).

Morris, J. T., Sundareshwar, P., & Nietch, C. (2002). Responses of coastal wetlands to rising sea level. *Ecology*, *83*(10), 2869–2877.

Mudd, S. M., Fagherazzi, S. , Morris, J. T. and Furbish, D. J. (2013). Flow, Sedimentation, and Biomass Production on a Vegetated Salt Marsh in South Carolina: Toward a Predictive Model of Marsh Morphologic and Ecologic Evolution. In The Ecogeomorphology of Tidal Marshes (eds S. Fagherazzi, M. Marani and L. K. Blum). doi:10.1029/CE059p0165

Najjar, R. G., Herrmann, M., Alexander, R., Boyer, E. W., Burdige, D. J., Butman, D., et al. (2018). Carbon Budget of Tidal Wetlands, Estuaries, and Shelf Waters of Eastern North America. *Global Biogeochemical Cycles*, 32. https://doi.org/10.1002/2017GB005790

NOAA National Estuarine Research Reserve System (NERRS). System-wide Monitoring Program. Data accessed from the NOAA NERRS Centralized Data Management Office website: http://www.nerrsdata.org/; accessed 12 October 2012.

Nuttle, W. K., & Hemond, H. F. (1988). Salt marsh hydrology: implications for biogeochemical fluxes to the atmosphere and estuaries. *Global Biogeochemical Cycles*, *2*(2), 91–114. https://doi.org/10.1029/GB002i002p00091

Odum, E.P. (1980). The status of three ecosystem-level hypotheses regarding salt marsh estuaries: tidal subsidy, outwelling, and detritus-based food chains. Estuarine Perspectives (Kennedy V.S., ed) Academic Press, New York. Pp. 485-495.

Ouyang, X., & Lee, S. Y. (2014). Updated estimates of carbon accumulation rates in coastal marsh sediments. *Biogeosciences*, *11*(18), 5057–5071. https://doi.org/10.5194/bg-11-5057-2014

Reed, D. J. (1995). The response of coastal marshes to sea-level rise: Survival or submergence? *Earth Surface Processes and Landforms*, *20*(1), 39–48. https://doi.org/10.1002/esp.3290200105

Rotzoll, K., & Fletcher, C. H. (2013). Assessment of groundwater inundation as a consequence of sea-level rise. *Nature Climate Change*, *3*(5), 477–481. https://doi.org/10.1038/nclimate1725

Sawyer, A. H., Michael, H. a., & Schroth, A. W. (2016). From soil to sea: the role of groundwater in coastal critical zone processes. Wiley Interdisciplinary Reviews: Water, 3(October). https://doi.org/10.1002/wat2.1157

Schaap, M. G., & Leij, F. J. (2000). Improved prediction of unsaturated hydraulic conductivity with the Mualem-van Genuchten model. *Soil Science Society of America Journal*, 65, 843–851.

Schlesinger, W. H. (1997). *Biogeochemistry: an analysis of global change* (2nd edn.). San Diego, CA: Academic Press.

Siok, D., (2017). 2017 Surface Elevation Table Annual Report. Dover, Delaware: Delaware National Estuarine Research Reserve.

Smith, J. A. M. (2013). The Role of Phragmites australis in Mediating Inland Salt Marsh Migration in a Mid-Atlantic Estuary. *PLoS ONE*, *8*(5). https://doi.org/10.1371/journal.pone.0065091

Soil Survey Staff, Natural Resources Conservation Service, United States Department of Agriculture. Web Soil Survey. Available online at the following link: https://websoilsurvey.sc.egov.usda.gov/.

Stahl, M. O., Tarek, M. H., Yeo, D. C. J., Badruzzaman, A. B. M., & Harvey, C. F. (2014). Crab burrows as conduits for groundwater-surface water exchange in Bangladesh. *Geophysical Research Letters*, 41(23), 8342–8347. https://doi.org/10.1002/2014GL061626

Teal, J. M. (1958). Distribution of Fiddler Crabs in Georgia Salt Marshes. *Ecology*, 39(2), 185–193. https://doi.org/10.2307/1931862

Teal, J. M., & Kanwisher, J. W. (1970). Total Energy Balance in Salt Marsh Grasses. Ecology, 51(4), 690–695.

Therrien, R., R. G. McLaren, E. A. Sudicky, and S. M. Panday (2006), HydroGeoSphere: A Three-Dimensional Numerical Model Describing Fully- Integrated Subsurface and Surface Flow and Solute Transport, 349 pp., Groundwater Simul. Group, Waterloo, Ontario.

Thorne, K., Macdonald, G., Guntenspergen, G., Ambrose, R., Buffington, K., Dugger, B., et al. (2018). U . S . Pacific coastal wetland resilience and vulnerability to sea-level rise. *Science Advances*, (4), 1–11. https://doi.org/10.1126/sciadv.aao3270

Tucker, K. (2016). *Variability of organic carbon accumulation on a tidal wetland coast*. Master's thesis. Lewes, Delaware: University of Delaware.

Valiela, I., Lloret, J., Bowyer, T., Miner, S., Remsen, D., Elmstrom, E., et al. (2018). Transient coastal landscapes: Rising sea level threatens salt marshes. *Science of the Total Environment*, *640–641*, 1148–1156. https://doi.org/10.1016/j.scitotenv.2018.05.235

Wang, Z. A., Kroeger, K. D., Ganju, N. K., Gonneea, M. E., & Chu, S. N. (2016). Intertidal salt marshes as an important source of inorganic carbon to the coastal ocean. *Limnology and Oceanography*, *2*(Dic), 1916–1931. https://doi.org/10.1002/lno.10347

Wasson, K., Raposa, K., Almeida, M., Beheshti, K., Crooks, J. A., Deck, A., … Guy, R. (2019). Pattern and scale: evaluating generalities in crab distributions and marsh dynamics from small plots to a national scale. *Ecology*, 100(10), 1–17. https://doi.org/10.1002/ecy.2813

Wilson, A. M., & Gardner, L. R. (2006). Tidally driven groundwater flow and solute exchange in a marsh: Numerical simulations. *Water Resources Research*, 42(1), 1–9. https://doi.org/10.1029/2005WR004302

Wilson, A. M., & Morris, J. T. (2012). The influence of tidal forcing on groundwater flow and nutrient exchange in a salt marsh-dominated estuary. *Biogeochemistry*, *108*(1–3), 27–38. https://doi.org/10.1007/s10533-010-9570-y

Wilson, A. M., Evans, T., Moore, W., Schutte, C. A., Joye, S. B., Hughes, A. H., & Anderson, J. L. (2015a). Groundwater controls ecological zonation of salt marsh macrophytes. *Ecology*, *96*(3), 840–849. https://doi.org/10.1890/13-2183.1.sm

Wilson, A. M., Evans, T. B., Moore, W. S., Schutte, C. A., & Joye, S. B. (2015b). What time scales are important for monitoring tidally influenced submarine groundwater discharge? Insights from a salt marsh. *Water Resources Research*, *51*, 4198–4207. https://doi.org/10.1002/2014WR016259

Xiao, K., Li, H., Wilson, A. M., Xia, Y., Wan, L., Zheng, C., et al. (2017). Tidal groundwater flow and its ecological effects in a brackish marsh at the mouth of a large sub-tropical river. *Journal of Hydrology*, 555, 198–212. https://doi.org/10.1016/j.jhydrol.2017.10.025

Xiao, K., Wilson, A. M., Li, H., & Ryan, C. (2019). Crab burrows as preferential flow conduits for groundwater flow and transport in salt marshes: A modeling study. *Advances in Water Resources*, 132(June), 103408. https://doi.org/10.1016/j.advwatres.2019.103408

Xin, P., Gibbes, B., Li, L., Song, Z., & Lockington, D. (2010). Soil saturation index of salt marshes subjected to spring-neap tides: a new variable for describing marsh soil aeration condition. *Hydrological Processes*, 24(18), 2564–2577. https://doi.org/10.1002/hyp.7670

Xin, P., Jin, G., Li, L., & Barry, D. a. (2009). Effects of crab burrows on pore water flows in salt marshes. *Advances in Water Resources*, 32(3), 439–449. https://doi.org/10.1016/j.advwatres.2008.12.008

Xin, P., Kong, J., Li, L., & Barry, D. A. (2013). Modelling of groundwater-vegetation interactions in a tidal marsh. *Advances in Water Resources*, *57*(April), 52–68. https://doi.org/10.1016/j.advwatres.2013.04.005

Xin, P., Yuan, L. R., Li, L., & Barry, D. a. (2011). Tidally driven multiscale pore water flow in a creek-marsh system. *Water Resources Research*, 47(7), 1–19. https://doi.org/10.1029/2010WR010110

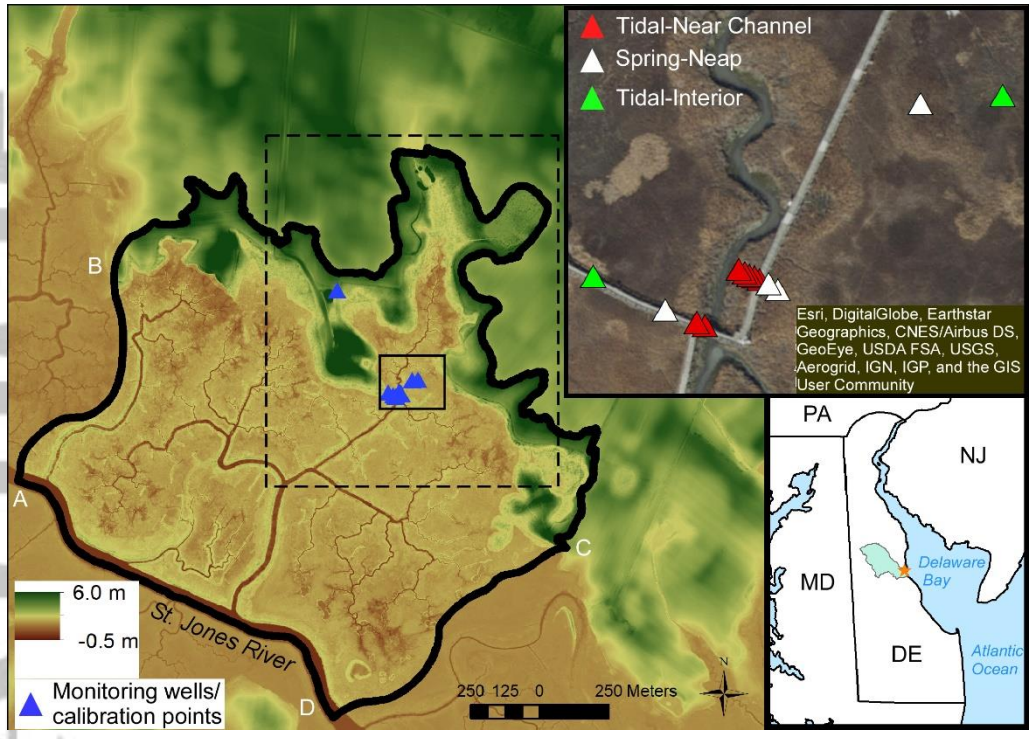


Figure 1. Map view of topography in model domain and surrounding area and model calibration points. The DEM within the model domain has been corrected for vegetation bias. Elevation is relative to NAVD88. Solid black box outlines the area in which marsh field data for calibration was collected. Dashed box indicates where delineation of hydrologic zones from the model output was analyzed. Top right: close-up of monitoring wells/calibration points and their respective hydrologic zones. Bottom right: Orange star shows model location with respect to the Delaware Bay, Atlantic Ocean, and surrounding states. Green area is St. Jones River watershed.

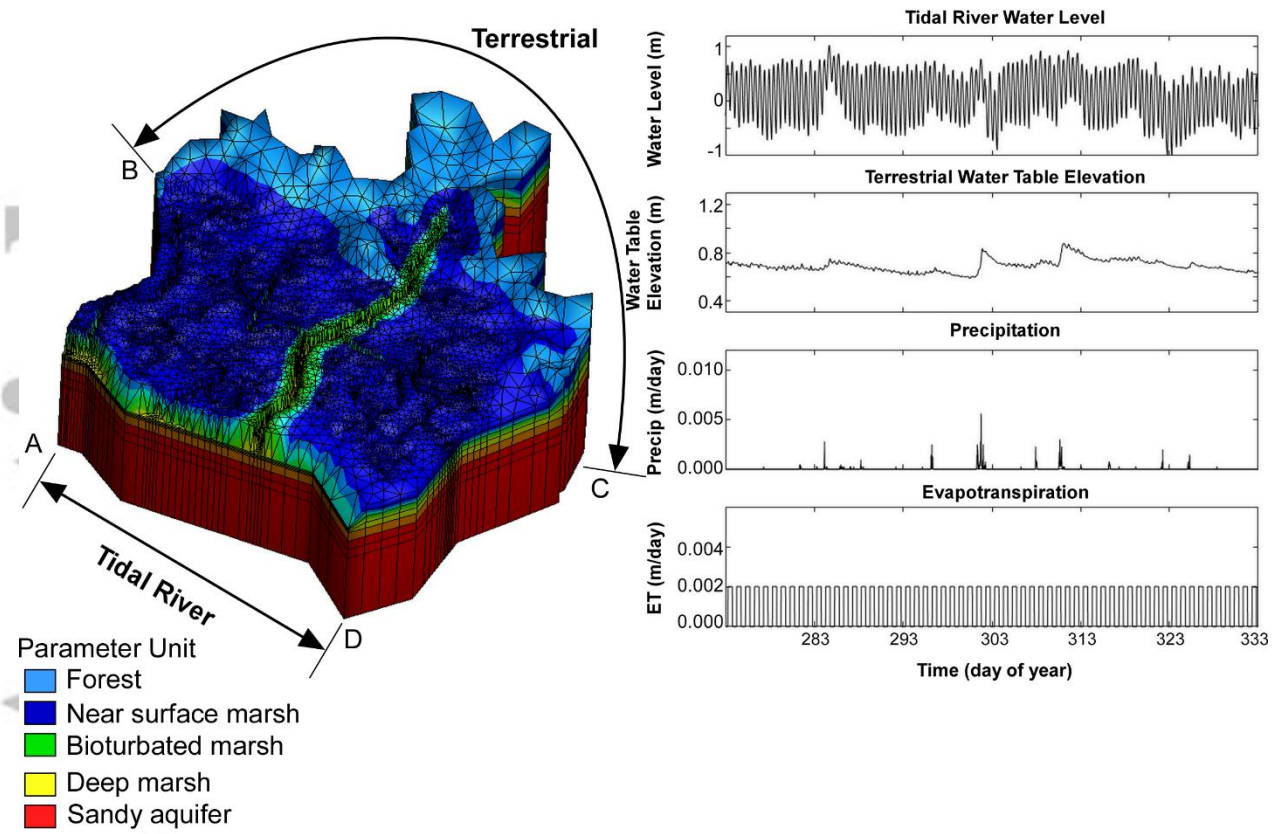


Figure 2. Subsurface model domain and mesh with delineation of parameter units and location of subsurface boundary conditions. ABCD are used to delineate boundary conditions. All boundary conditions with time for October-November 2017 are shown on the right. Figures S5 and S6 show boundary conditions for July-September 2017 and March-April 2018.

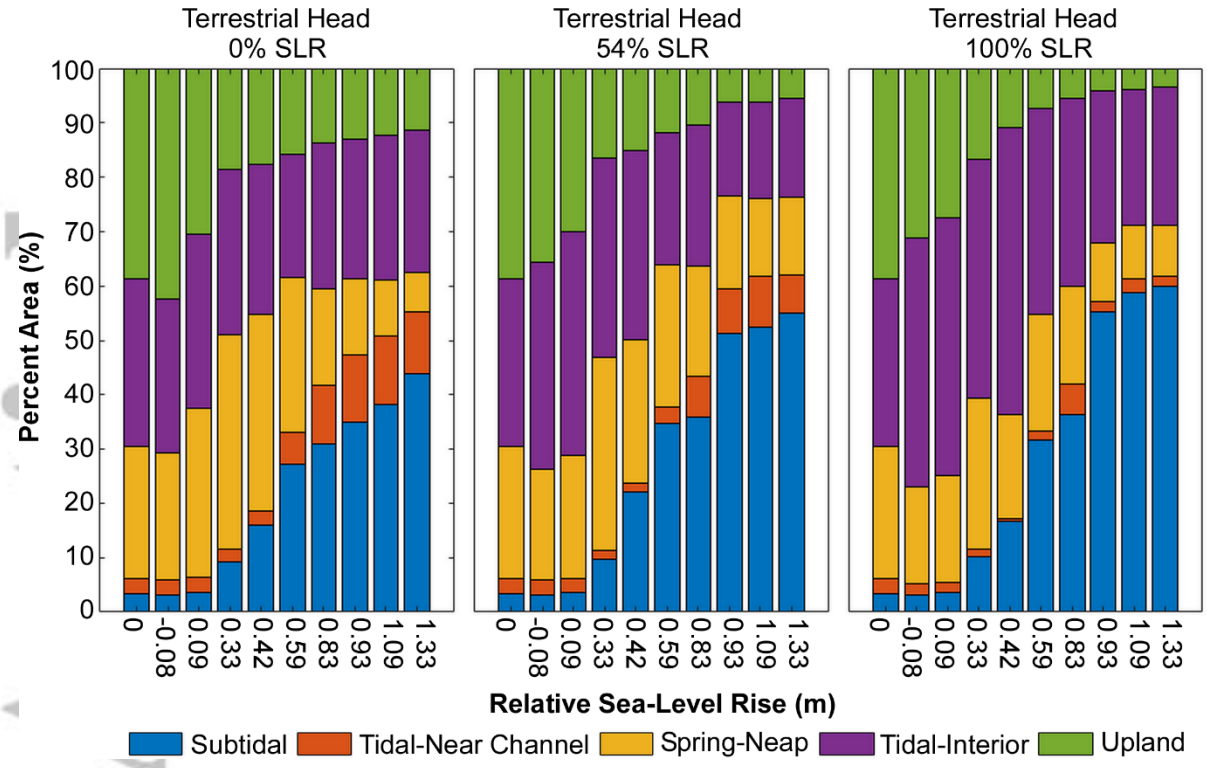


Figure 3. Percent of the total marsh area occupied by each hydrologic zone for all RSLR and terrestrial head scenarios. While general trends are similar, results highlight differences in zone area between terrestrial conditions. Note that the difference in RSLR between adjacent bars is not consistent.

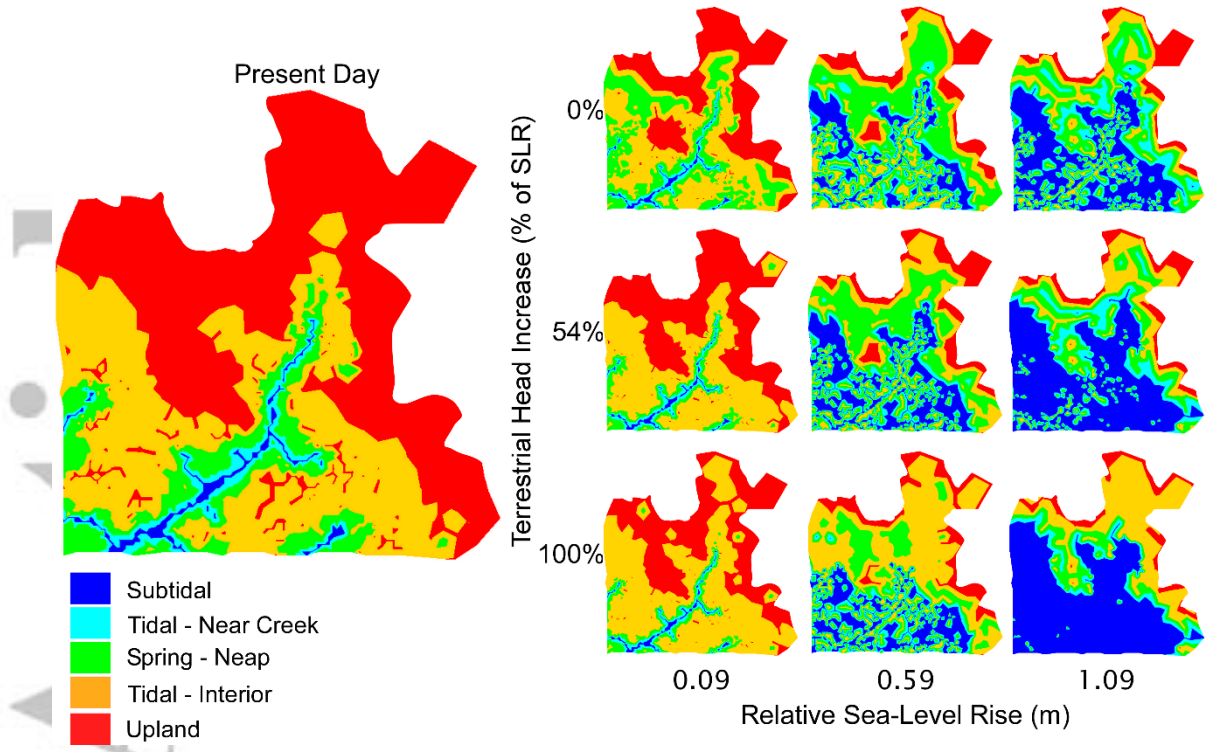


Figure 4. Map of hydrologic zones under 0, 0.9, 0.59, and 1.09 m of RSLR for each terrestrial head scenario for the October-November 2017 simulation. Mapped results from the February-March and July-September 2018 time periods are shown in Figures S7 and S8. See Text S3 for discussion of seasonal differences in zonation patterns.

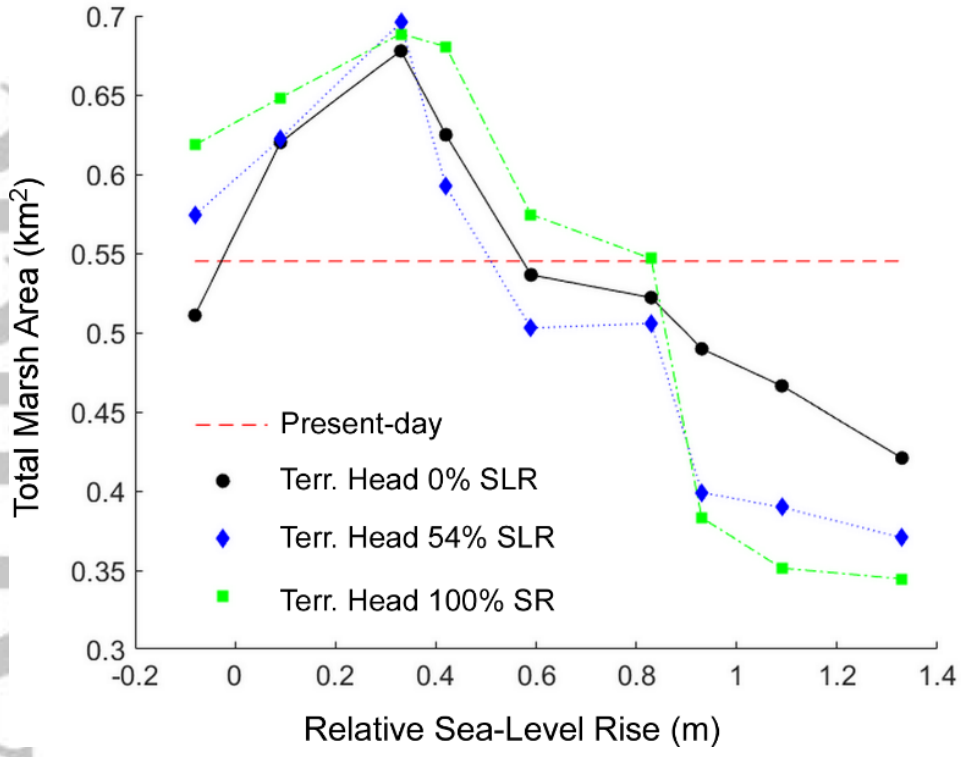


Figure 5. Total marsh area, quantified as the sum of the tidal-near channel, spring-neap, and tidal-interior zones, with RSLR for all terrestrial head scenarios. Terr. Head = Terrestrial Head.

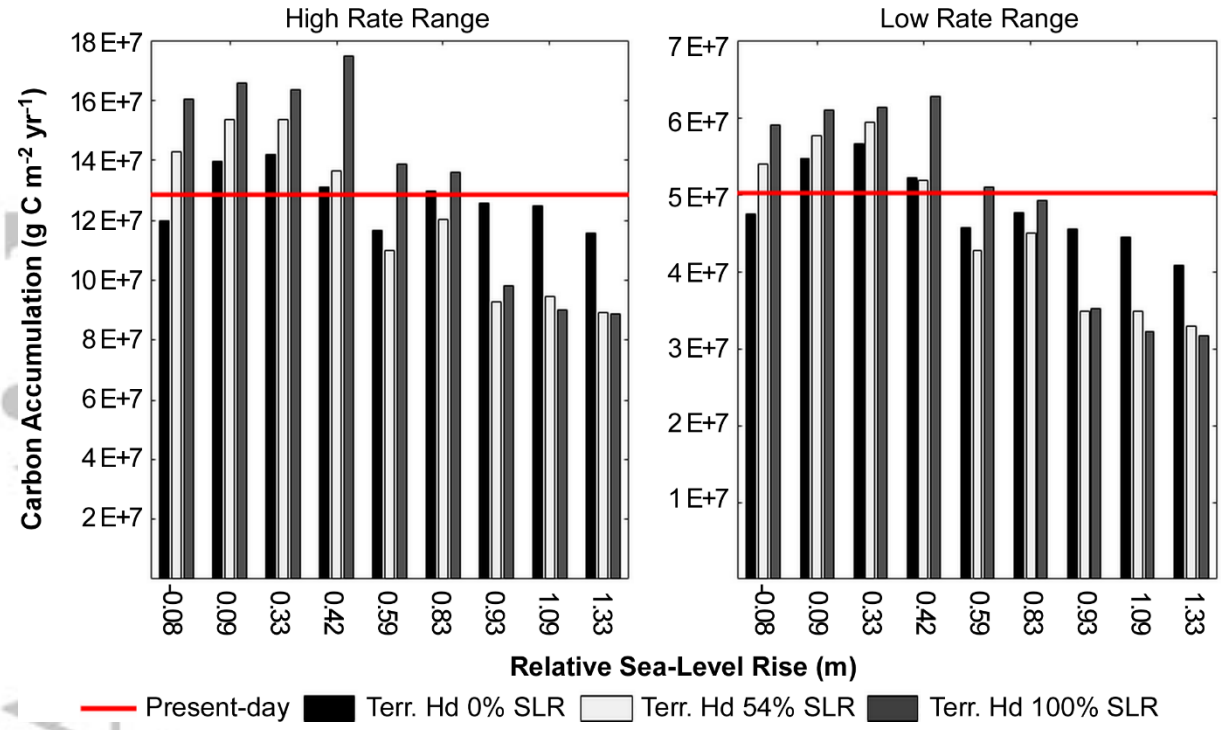


Figure 6. Total carbon accumulation in sub-domain area for all RSLR and terrestrial head conditions for high and low carbon accumulation rates (Table 2). Terr. Hd = Terrestrial Head.

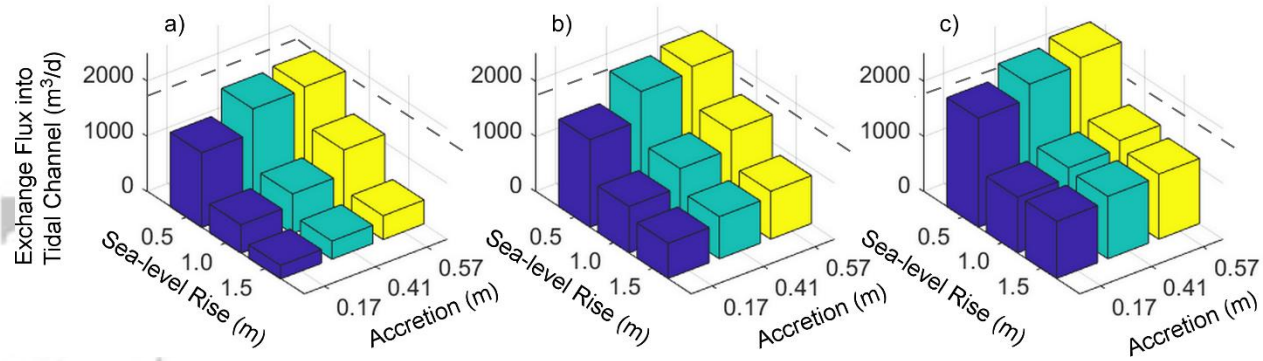


Figure 7. Exchange flux from the marsh platform into the tidal channel for all SLR and sediment accretion scenarios with a) terrestrial head equivalent to present-day across scenarios, b) terrestrial head increase 54% of SLR, and c) terrestrial head increase equal to SLR. Grey dashed line is present-day flux.

Table 1. Porous media and overland flow model parameters by unit.

| **Parameter** | **Value** | | | | | **Source** |
|---|---|---|---|---|---|---|
| **Porous media** | Forest | Bioturbated Marsh* | Near surface Marsh | Deep Marsh | Sandy Aquifer | |
| | variable (~1.0 m) | variable (~0.25 m) | | | | |
| Hydraulic conductivity (m $d^{-1}$)† | 5[1,4] | 0.03[2] | 0.009[2] | 0.005[2] | 60[3] | 1) Loheide et al., 2005; 2) Guimond et al., in review; 3) He & McKenna, 2014; 4) USDA |
| Porosity | 0.4[1] | 0.4[1] | 0.4[1] | 0.4[1] | 0.5[3] | 1) Loheide et al., 2005; 2) Schaap, 2000; 3) Xin et al., 2010 |
| Van Genuchten α ($m^{-1}$)† | 2.6[2] | 5.9[1] | 5.9[1] | 5.9[1] | 14.5[1] | |
| Van Genuchten β† | 1.6[2] | 1.48[1] | 1.48[1] | 1.48[1] | 2.68[1] | |
| Residual Saturation | 0.15 | 0.15 | 0.15 | 0.15 | 0.10 | Xin et al., 2010 |
| **Overland Flow** | Entire Domain | | | | | |
| Manning roughness coefficient (d $m^{-1/3}$) | $6x10^{-7}$ | | | | | Moffett et al., 2012 |
| rill storage height (m) | 0.002 | | | | | Moffett et al., 2012 |
| Surface -subsurface exchange coefficient | 0.001 | | | | | Moffett et al., 2012 |

* Bioturbated marsh region was only included in July-September 2018 simulations.

† Refined based on calibration.

Table 2. Observation well hydrograph analysis criteria for designation of hydrologic zone and assumed high and low carbon accumulation rates for each zone. M2 is the principal lunar tidal signal with a period of 12.42 hours.

| Hydrologic Zone | Criteria | | | Carbon Accumulation ($g\ C\ m^{-2}\ yr^{-1}$) | |
|---|---|---|---|---|---|
| | Oscillation | Inundation | Average Head | High | Low |
| Subtidal | M2 >=70 | 100% | | 0 | 0 |
| Tidal-Near Channel | M2 >=70 | <100% | Average depth to water >0.1m | 300[1] | 100[1,2] |
| Upland | | | Average depth to water >1m | 10[4] | 5[4] |
| Spring-Neap | Long Duration Harmonics >35 | <60% | | 130[1,3] | 65[1,3] |
| Tidal-Interior | M2 >= 20 | | | 300[1] | 100[1,2] |
| Upland | | <5% | | | |
| Tidal-Interior | | >= 5% | | | |

[1]Tucker (2016)
[2]Choi and Wang (2004)
[3]Ouyang & Lee (2014)
[4]Schlesinger (1997)